Electronic Supplementary Material (ESI) for Nanoscale.

Supplementary information.

1 Nanocrystals size distributions

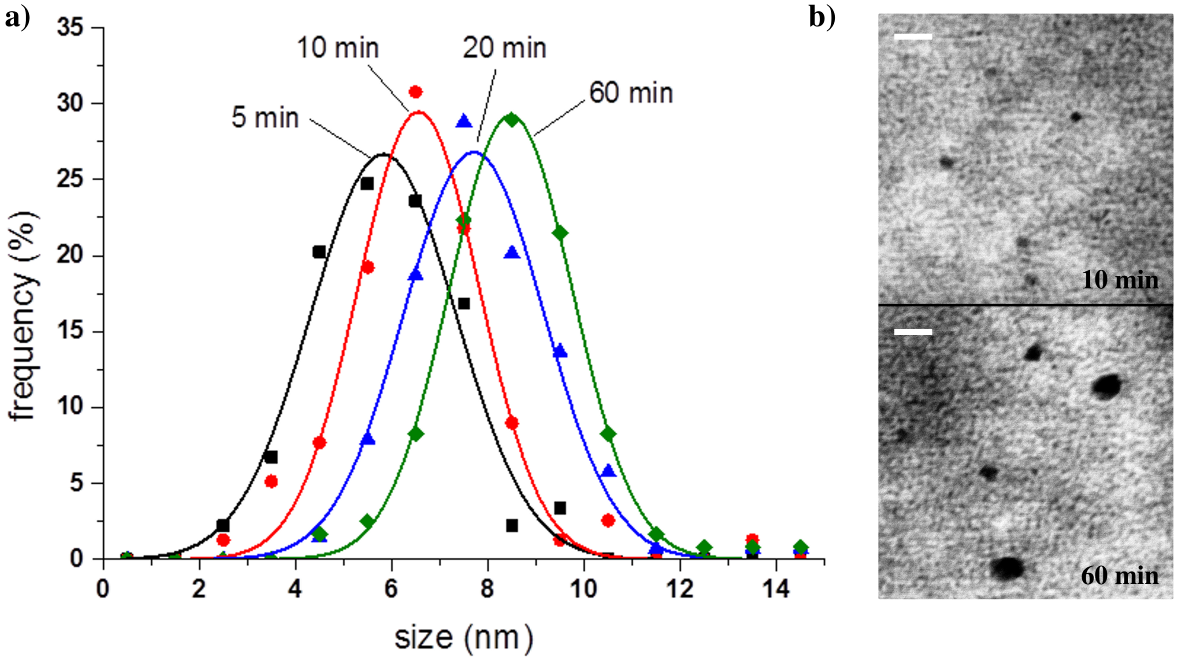

Fig. 1 a) Examples of size distribution functions of ZAIS nanocrystals obtained at different reaction times. b) Typical images of ZAIS nanocrystals obtained using scanning transmission electron microscopy (STEM) for reaction times of 5 and 60 min. Scale bars represent 20 nm.

$AgInS_2$-ZnS (ZAIS) nanocrystals synthesized using the procedure exposed in the article have a average size around 7-8 nm. However, as exposed in the last part of the article, this average size can be controlled from 5.8 nm to 8.6 nm by varying the reaction time. Images taken using scanning transmission electron microscopy (STEM) were used to measure the size of ZAIS nanocrystals using the ImageJ sofware[1]. With the measure of ∼200 nanocrystals, size distribution histograms could be created. The average size and size distribution were obtained by fitting these histograms with gaussian functions. Examples of these size distributions are presented in figure 1.

2 Photoluminescence quantum yields

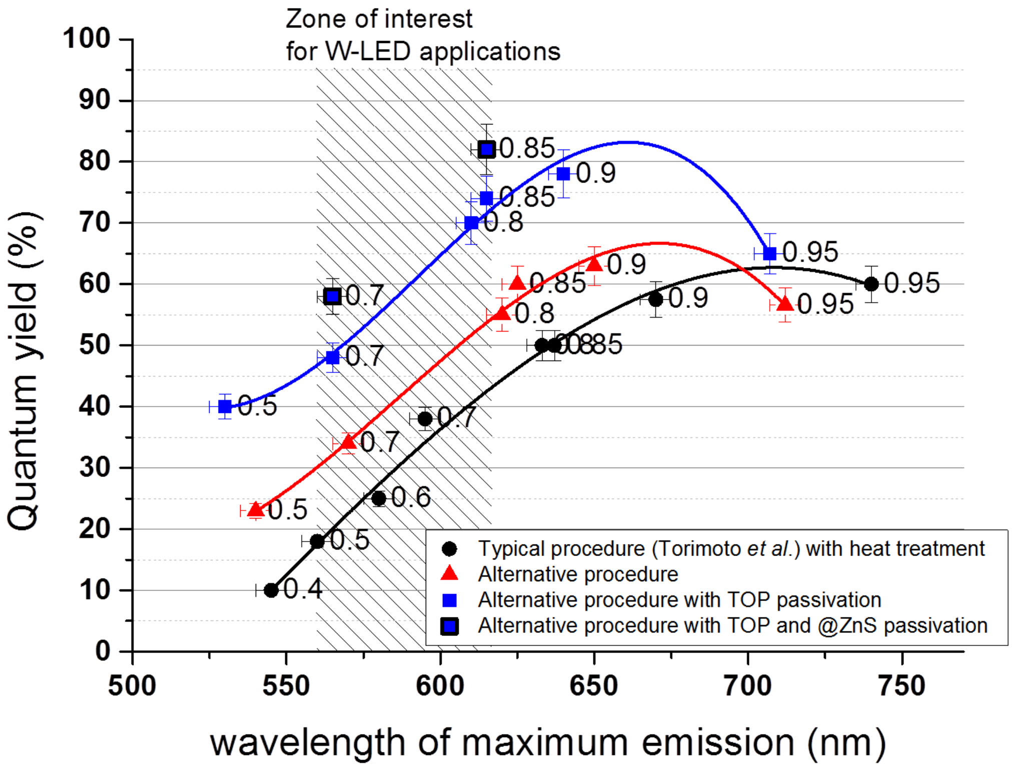

Fig. 2 photoluminescence quantum yield of ZAIS nanocrystals using different precursor compositions and synthesis procedures

The composition X of the precursor $((AgIn)_X Zn_{2-2X}(S_2CN(C_2H_5)_2)_4)$ is the major parameter controlling the composition of the resulting ZAIS nanocrystals. Photoluminescence spectrum and photoluminescence quantum yield of the ZAIS nanocrystals depend strongly on their composition. The figure 2 shows the absolute quantum yield obtained with different precursor composition X using classic and modified procedures as a function of their maximum emission wavelengths. Thanks to effective passivation of non-radiative surface defects by trioctylophosphine , quantum yields up to 80% were reached without the addition of ZnS shell. With our new synthesis procedure, the quantum yield of yellow emitting nanocrystals was increased from $\sim 30\%$ to $\sim 60\%$.

3 Determination of band gap and Urbach energies

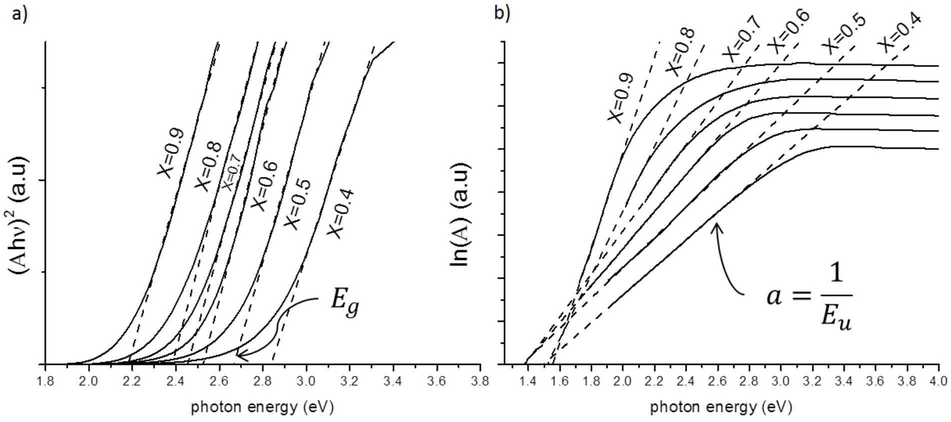

Fig. 3 Characterization of the absorption near the band edge of ZAIS nanocrystals. a) measure of the optical band gap and b) Urbach energies for nanocrystals synthesized with different composition X of precursor

The optical absorption of ZAIS nanocrystals colloidal solutions was measured in the integrating sphere of the photoluminescence quantum yield spectrometer. The Tauc formula for a direct band gap[2,3] was used to extract the value of the optical band gap of each nanocrystals composition.

$$A.h\nu \propto (h\nu - E_g)^2 \qquad \text{for } h\nu > E_g \tag{1}$$

where A is the measured absorption and E_g is the direct band gap of the semiconductor.

For photon energies below the band gap, the absorption is modeled by the Urbach tail of formula[4]:

$$A \propto exp(h\nu / E_u) \qquad \text{for } h\nu < E_g \tag{2}$$

where E_u is the Urbach energy which is extracted from the inverse of the slope of the ln(A) vs hν curve. examples are shown in figure 3.

4 Fitting method for time-resolved emission spectroscopy

The choice of the fitting method used to interpret the time evolution of the intensity signals was based on the one presented J.R. Lakowicz[5]. This methods relies in part on the statistical analysis provided by the χ^2 test which necessits the knowledge of the standard deviation of the measurement.

As explained in the full article, correct values of the reduced χ^2 could only be found using a 3-exponential fitting function. However, the validity of such model can also be assesed using residual plots. Indeed, an inapropriate fitting function results in large oscilations on the residual plots. Such behavior can be clearly observed when using a 2-exponential fitting function (see fig.4b)). This confirms the fact that the photoluminescence process cannot be explained by only two recombnaison processes.

A similar, although less pronouced, behavior is observed when using a stretched-exponential decay. However, a 3-exponential fit induces no flutations redices the spread of the error to a value that can be explained by the experimental measurement error (*ie*. the reduced χ^2 is almost equal to 1)

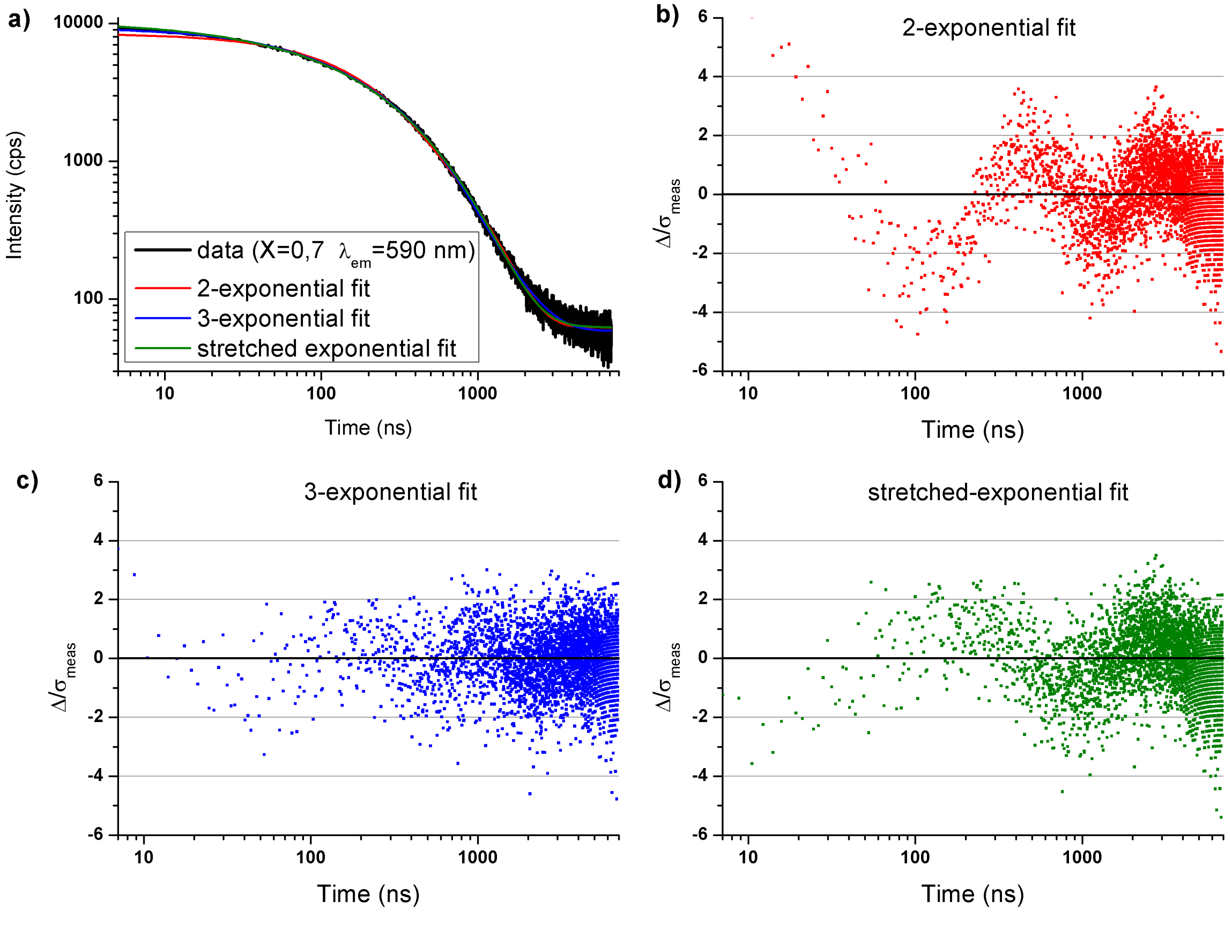

Fig. 4 exemple showing the typical outcomes of the fiting procedure using different fitting functions. a) plot of the raw data and fitted functions. The residuals (Δ) normalised by the known experimental error (σ_{meas}) are plotted for b) a 2-exponential fit, c) a 3-exponential fit and d) a stretched-exponential fit.

5 Lifetimes and proportions of each recombination pathways for three compositions

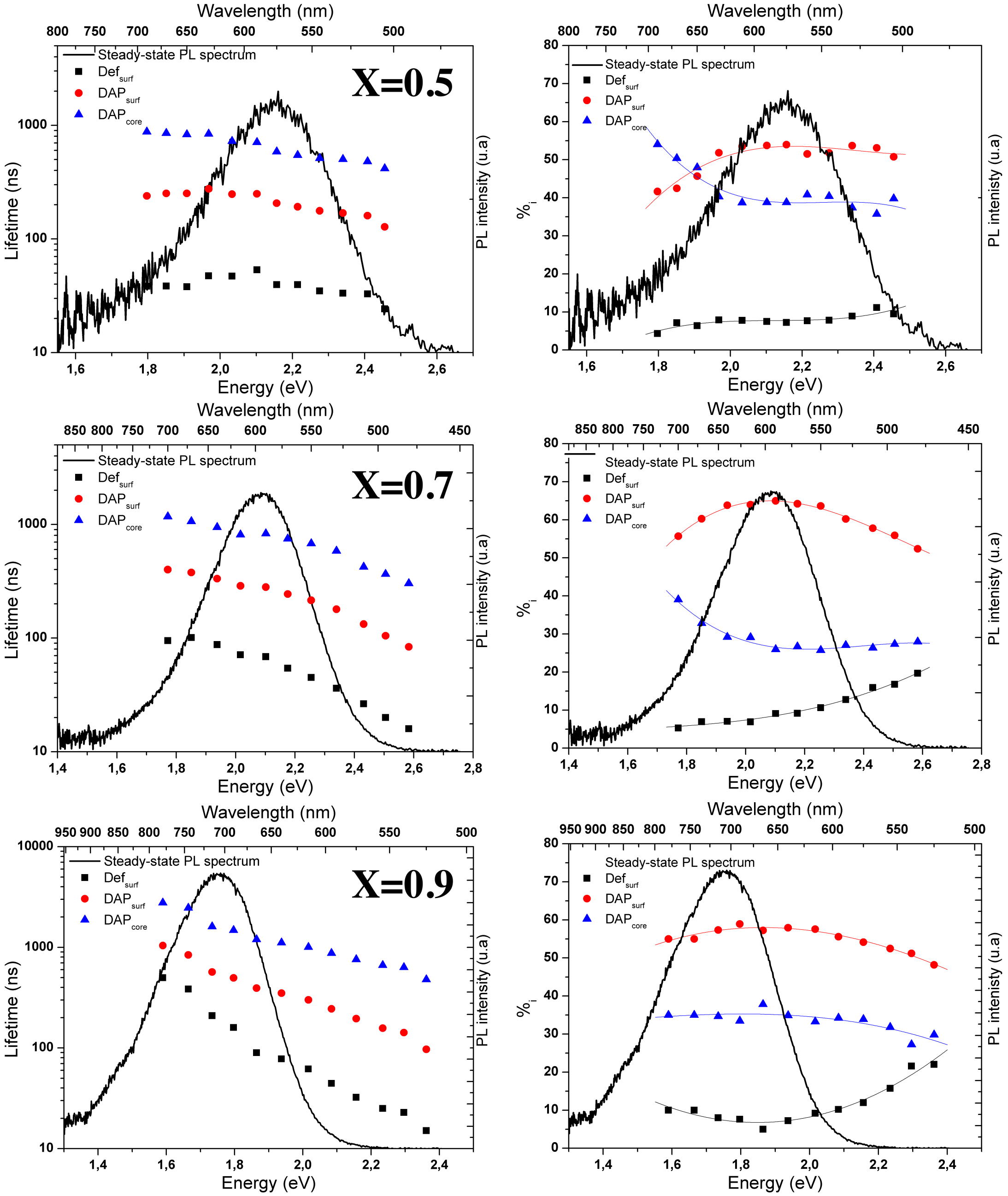

Fig. 5 Extracted fluorescence lifetimes and proportion for the three recombination pathways for nanocrystals synthesized with a precursor composition X=0.5

6 Construction of each contributions spectrum

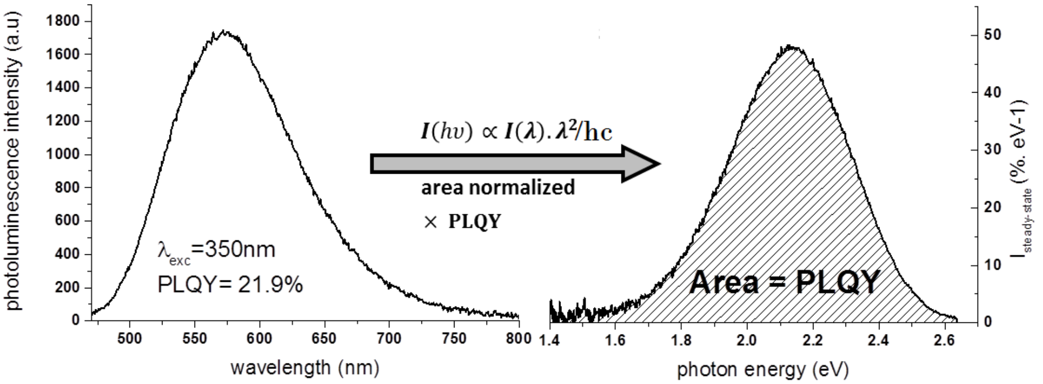

Fig. 6 Construction of the quantitative steady-state spectrum using quantum yield measurements

First, photoluminescence spectra recorded in the integrated sphere were represented on the energy scale using the needed Jacobian transformation[6] :

$$I_E(h\nu) = I_\lambda.\lambda^2/hc \tag{3}$$

Where I_E and I_λ are the fluorescence intensity in the nergy and wavelength spaces respectively.

Then, for a given excitation wavelength, the emission spectrum was area-normalized and multiplied by its measured absolute quantum yield so that the integral of the resulting emission spectrum $I_{steady-state}(h\nu)$ corresponds to its quantum efficiency. This spectrum is therefore the probability density function of radiative recombination. This process is summarized in the figure 6.

In a second step, the TRES signals for several emission wavelengths of the photoluminescence spectrum were fitted with a triple-exponential function as explained in the main article.

$$I(t,\lambda) = A_1\exp(\frac{-t}{\tau_1}) + A_2\exp(\frac{-t}{\tau_2}) + A_3\exp(\frac{-t}{\tau_3}) \tag{4}$$

The steady-state intensity $I_{steady-state}$ at a given emission wavelength λ is therefore proportional to :

$$\int_{t=0}^{\infty} I(t,\lambda)\mathrm{d}t = A_1\tau_1 + A_2\tau_2 + A_3\tau_3 \tag{5}$$

Where the τ_i are the photoluminescence lifetimes of each recombination paths. The proportion of the steady-state intensity originating from the recombination process i is then :

$$\%_i(h\nu) = \frac{A_i\tau_i}{\sum_{i=1}^{3} A_i\tau_i} \qquad \text{for i=1, 2 or 3} \tag{6}$$

Finally, the quantitative intensity of a recombination process is obtained by multiplying its proportion $\%_i$ with the global intensity $I_{steady-states}$. By repeating this approach on different emission wavelengths, three photoluminescence spectra associated with each of the three recombination processes are constructed.

$$\begin{aligned} I_{steady-state}(h\nu) &= I_1(h\nu)+I_2(h\nu)+I_3(h\nu) \\ \text{where : } I_i(h\nu) &= \%_i(h\nu).I_{steady-state}(h\nu) \qquad \text{for i=1, 2 or 3} \end{aligned} \tag{7}$$

The partial spectra $I_i(h\nu)$ are therefore representations of both the line-shapes and efficiencies of each photoluminescence process.

References

1 W. S. Rasband, *Image J*, U.S National Intitutes of Health, Betesda, Maryland, USA, http://imagej.nih.gov/ij/, 1997.

2 J. Tauc and A. Menth, *Journal of Non-Crystalline Solids*, 1972, **8-10**, 569–585.

3 N. Ghobadi, *International Nano Letters*, 2013, **3**, 2.

4 F. Urbach, *Physical Review*, 1953, **92**, 1324–1324.

5 *Principles of Fluorescence Spectroscopy*, ed. J. R. Lakowicz, Springer US, Boston, MA, 2006.

6 J. Mooney and P. Kambhampati, *The Journal of Physical Chemistry Letters*, 2013, **4**, 3316–3318.